High-field magnetooptical behavior of polymer-embedded single-walled carbon nanotubes

A. Nish,[1] R. J. Nicholas,[1,*] C. Faugeras,[2] Z. Bao,[2] and M. Potemski[2]
[1]*Department of Physics, Clarendon Laboratory, University of Oxford, Parks Road, Oxford, 0X1 3PU, United Kingdom*
[2]*Laboratoire de Champs Magnétiques Intenses, 25 Ave des Martyrs, BP166, 38042 Grenoble, France*
(Received 10 October 2008; published 10 December 2008)

We report a study of the magnetophotoluminescence (PL) of single-walled carbon nanotubes embedded in polymer films. The magnetic-field dependence of the intensity and emission energy is used to deduce the splitting and mixing of the bright and dark exciton states. It is shown that the presence of strain in the films causes a considerable increase in the bright–dark exciton splitting. The unstrained nanotubes show considerably smaller exciton splittings than reported previously and demonstrate an unexpected magnetic suppression of the PL intensity which can only be observed once the Aharanov-Bohm phase splitting is significantly larger than the bright–dark exciton splitting. Functional fitting of the data also allows the diameter dependence of the Aharanov-Bohm (AB) phase-induced energy shifts to be accurately measured. Evidence is also presented for the existence of a zero-field AB splitting due possibly to spin-orbit interaction effects.

DOI: 10.1103/PhysRevB.78.245413 PACS number(s): 78.67.Ch, 71.35.Ji

I. INTRODUCTION

The optical and magnetooptical properties of single-walled carbon nanotubes (SWNTs) have been a topic of intense interest in recent years particularly since it has been shown that their optical properties are dominated by excitonic effects. Their one-dimensional nature led to the prediction of large exciton binding energies of order of 0.5 eV,[1–4] which were found to agree well with experimental results where binding energies of order of 300–400 meV are seen for SWNTs with diameters of ~0.8 nm.[5–8] Detailed descriptions of the excitonic states are however quite complex because the electron and hole spins, combined with the presence of two valleys at the K and K' points of the Brillouin zone, lead to an exciton degeneracy of 16 of which only *one* state—the spin singlet of odd parity—is expected to be optically active ("bright").[9] The even-parity triplet states are lowest in energy and have been assumed to be optically inactive. The singlet state is split due to the interactions between the different valleys with the ordering and relative energy of the splittings being dependent on the details of the Coulomb interactions.[10–12] In the absence of any mixing terms, the lowest singlet level is the valley antibonding state which is dark but is predicted to be close in energy to the optically active (bright) bonding exciton state although there has been a recent report of other weakly active dark states[13] 40–100 meV lower in energy. Evidence for the very small energy difference between the bright and dark singlet states has been presented recently by a number of authors from studies of temperature[14] and magnetic-field dependences[15,16] of the emission intensities.

The magnetic-field effects are caused by applying an external magnetic field (B) parallel to the tube axis which adds an Aharanov-Bohm (AB) phase (ϕ) to the electron wave function in the circumferential direction. This shifts the band gap by an amount

$$(\Delta_{AB}/E_g) = \pm (3\pi d^2 B/4\phi_0) \quad (1)$$

for a SWNT of band gap E_g and diameter d lying parallel to an applied magnetic field B, where ϕ_0 $(=h/e)$ is the flux quantum.[17–19] We label this splitting as Ajiki-Ando (AA) splitting,[17] with the first evidence for its observation being reported by Zaric *et al.*[20] using very high magnetic fields to make measurements on solutions at high temperatures. The AB phase lifts the degeneracy of the K and K' states, which control the symmetry of the excitons. For sufficiently large AB flux,[9] the bonding and antibonding states are decoupled resulting in two bright exciton peaks, corresponding to the KK and $K'K'$ excitons, split by δE_g. This mechanism has been shown to be the origin of magnetic brightening observed in nanotubes at low temperatures[14–16,21] although the range of energy values deduced for the splitting of the bright and dark singlet states is quite large and showed a strong dependence on the chiral vector indices (n,m) and nanotube diameter (d).

Here we present studies of the magnetic-field dependence of photoluminescence (PL) intensities and energies for nanotubes which are encapsulated in polymers. The magnitudes of the exciton splittings are shown to be strongly dependent on the diameter and strain state of the nanotubes, with the splitting becoming smaller in the limit of less strain and larger diameter. This allowed us to reach the high-field limit of single valley exciton states where we found that there is an unexpected behavior which corresponds to a strong-field induced decrease in the PL efficiency.

II. EXPERIMENTAL METHODS

In order to provide a wide range of diameters for our study, SWNTs produced by the HiPCO (Carbon Nanotech.) growth technique were used in conjunction with the nonselective wrapping polymer, MEHPPV (American Dye Source). The preparation method for SWNTs with organic polymers has been described previously.[22–24] For this set of experiments, the optimal solvent for the solution dispersions was found to be o-xylene (Sigma-Aldrich). The samples were then prepared in two different ways from the same starting solution.

In the first method the MEHPPV-HiPCO was dried by repeatedly dropping a small volume of the solution onto a thin glass substrate. This produced a thick deposit which contained the nanotubes randomly orientated in the amor-

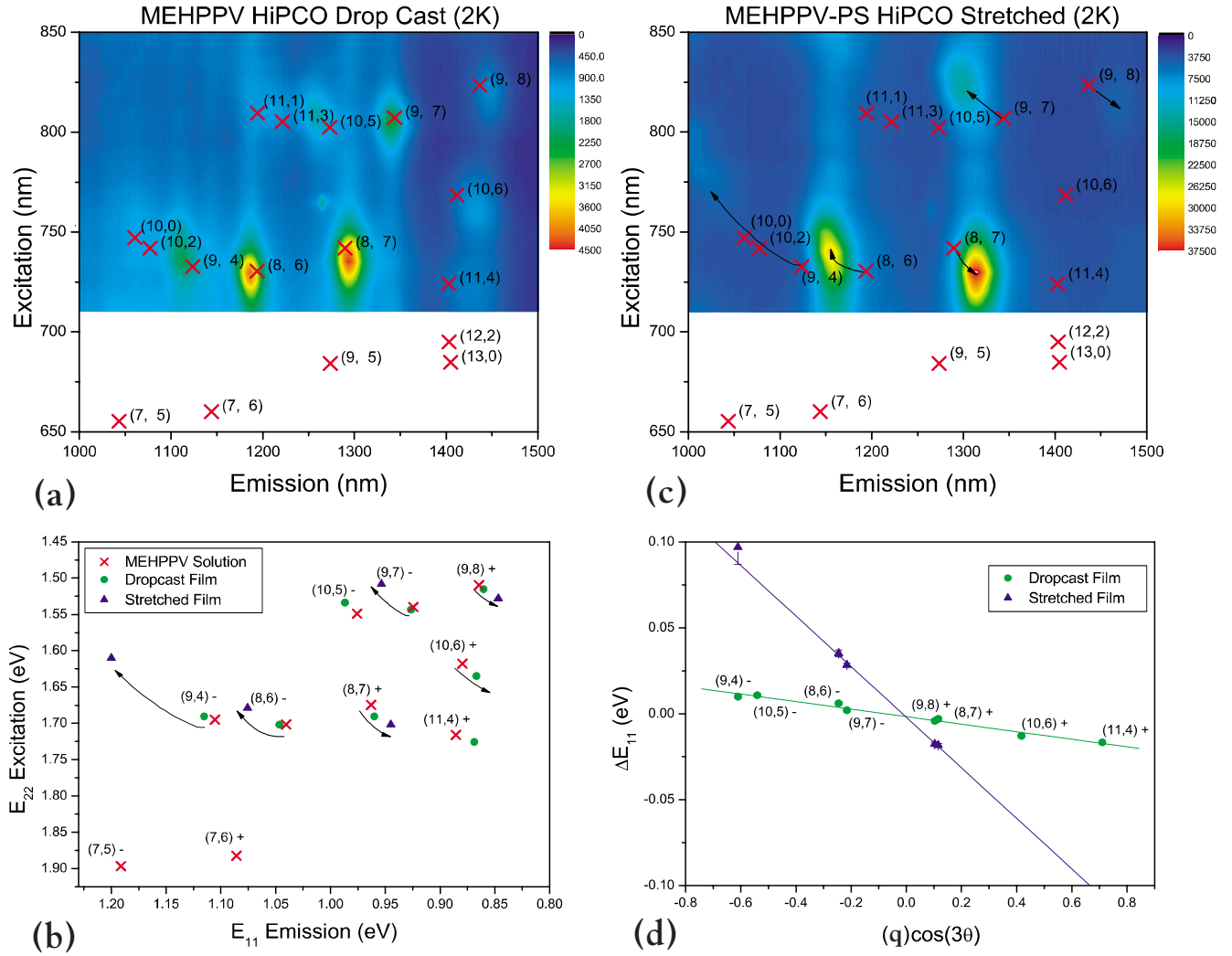

FIG. 1. (Color online) Parts (a) and (b) show PLE maps from Ti:sapphire excited tube species for both film samples at 2 K. The red crosses represent the positions of the (n,m) indexed SWNT peaks in MEHPPV-solvent solution. Arrows indicate the shifts in the transitions due to strain. These shifts are shown on an energy scale in part (c). Part (d) shows the dependence of the E_{11} transition on the nanotube chiral angle θ.

phous polymer matrix. In the second case a second polymer (polystyrene) was added to the initial solution and the composite dried in a similar manner as before. It was then possible to align the nanotubes along a particular direction by removing the deposit from the substrate and stretching it along one direction.[25] These films were thicker and more robust and could be stretched by up to a factor of 5 at ~370 K. The increased alignment of the SWNTs in the polymer matrix was verified using polarized PL spectroscopy.

Photoluminescence-excitation (PLE) maps were taken for each of the samples at 2 K showing the distinctive peaks corresponding to nanotube E_{11}-E_{22} resonances. Excitation was made in the range of 710–850 nm using a tunable Ti:sapphire laser and in the range of 610–660 nm using a tunable dye laser. Typical estimated output powers illuminating the sample were in the region of 1 mW. Collection was made through an optical fiber bundle with a liquid nitrogen cooled InGaAs array detector and 0.3 m spectrometer. Measurements of the field dependence were made in the Voigt geometry using polarizers mounted adjacent to the samples both parallel and perpendicular to the field for light propagating perpendicular to the field direction. Both exciting and emitted radiations are polarized giving an added selectivity to the orientation of the SWNTs which are probed. Optical absorption and emission in carbon nanotubes are strongly dependent upon the polarization of the incident light, with preferential absorption observed at the primary band gaps for light polarized parallel to the tube axis.[26,27]

Continuous fields of up to 32 T were provided by a 24 MW resistive-coil magnet at the Grenoble High Magnetic Field Laboratory. A variable-temperature insert inside the magnet bore allowed control of the temperature from 2 to 280 K.

III. RESULTS

Figure 1 shows PLE maps measured for the two different preparations of polymer wrapped nanotubes at 2 K in the region of 710–850 nm, which covers the majority of the

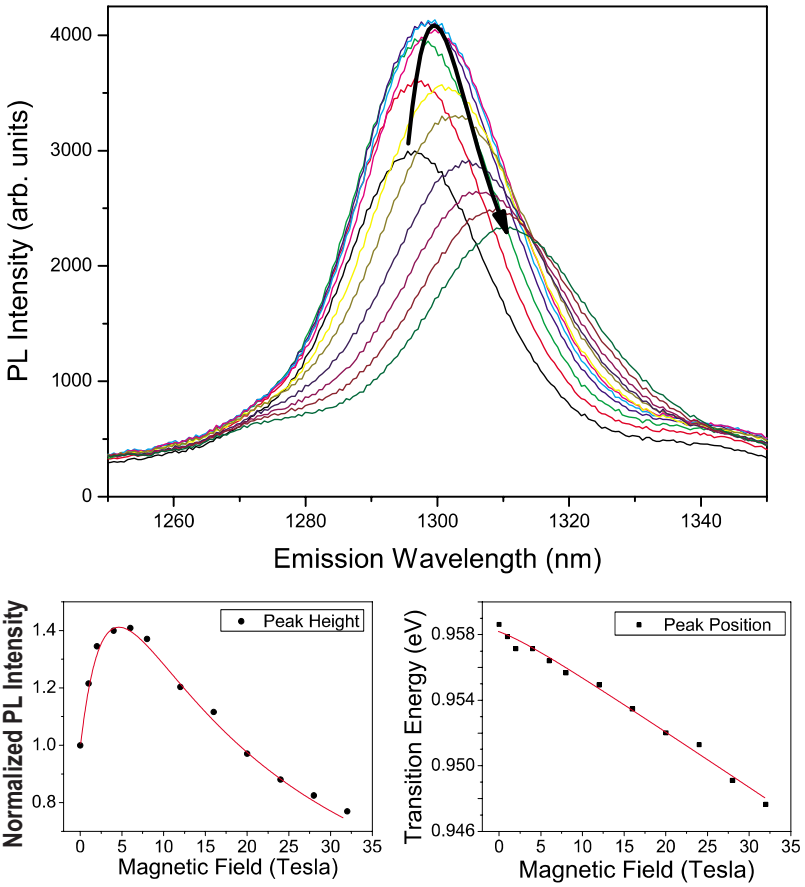

FIG. 2. (Color online) The PL peak of the (8,7) species in the unstrained drop-cast MEH-PPV film, as measured between 0 and 32 T. The lower figures show the separate behaviors of the amplitude and emission energy.

nanotube species present. The smaller diameter [(7,5) and (7,6)] species were probed using resonant excitation at around 660 nm from the dye laser. Shifts are observed in the positions of the transitions which are consistent with the family behavior that arises from the presence of a large uniaxial strain component.[28] This is most evident in the stretched polystyrene-MEHPPV/CNT film. The shifts may be analyzed using the expression for the strain induced band-gap shift ΔE_g^s following the theory of Yang and Han,[29] and as shown by Li *et al.*[30] and Leeuw *et al.*,[31]

$$\Delta E_g^s = 3q\gamma_0[(1+\nu)\sigma\cos(3\theta)], \tag{2}$$

where $q=\pm 1$ (from $n\text{-}m=3p+q$), γ_0 is the carbon-carbon transfer integral, ν is Poisson's ratio, σ is the strain along the nanotube axis, and θ is the chiral angle. Using this expression the shifts shown in Fig. 1 allow us to deduce relative levels of strain of 0.16% and 0.02% for the stretched polystyrene-MEHPPV film, and drop-cast MEHPPV film samples, respectively, at 2 K. Similar experiments on unstretched films containing polystyrene demonstrate that the strain is caused by the differential contraction in the polystyrene containing film and not by the stretching process. The strains should be compared with values of order of 0.25% as found in the quench frozen samples[30,32] used for our previous magneto-PL studies.[16]

Figure 2 shows a set of magneto-PL spectra for the (8,7) species for the drop-cast film where the polarized light selects tubes closest to parallel with the magnetic field. This shows a characteristic behavior in which there is a rapid initial magnetic brightening followed by a significant fall in intensity at high fields. The emission-peak position shows an almost linear decrease in energy at high field with field coefficient $\alpha=\frac{dE_g}{dB}$ meV/T. The experiments were repeated for light polarized perpendicular to the magnetic-field direction. For this case a similar magnetic brightening and shift of the emission energies was observed but with a considerably reduced field coefficient and a brightening which occurred at much larger magnetic fields, as illustrated in Fig. 3. This behavior is consistent with a much smaller AB flux threading the nanotubes which have been selected by this polarization due to their dominant orientation perpendicular to the magnetic field. When the experiments were performed with the polystyrene containing stretched and strained films, similar field coefficients were observed but the magnetic brightening effects were much larger and higher fields were required to observe the high field fall in intensity, consistent with our previous measurements on strained aqueous solutions[16] where only saturation was observed in larger diameter tubes studied up to 19.5 T.

We fit the magnetic brightening behavior using a conventional two level Hamiltonian analysis,[21]

$$\hat{H} = (\Delta_x/2)\hat{\sigma}_z + \Delta_{\mathrm{AB}}\hat{\sigma}_x, \tag{3}$$

where Δ_x is the dark–bright exciton splitting, Δ_{AB} is the Aharanov-Bohm shift, and $\hat{\sigma}_x$ and $\hat{\sigma}_z$ are the Pauli-spin matrices. In order to fit the observed behavior, however, it is necessary to introduce two additional factors. First, there is a

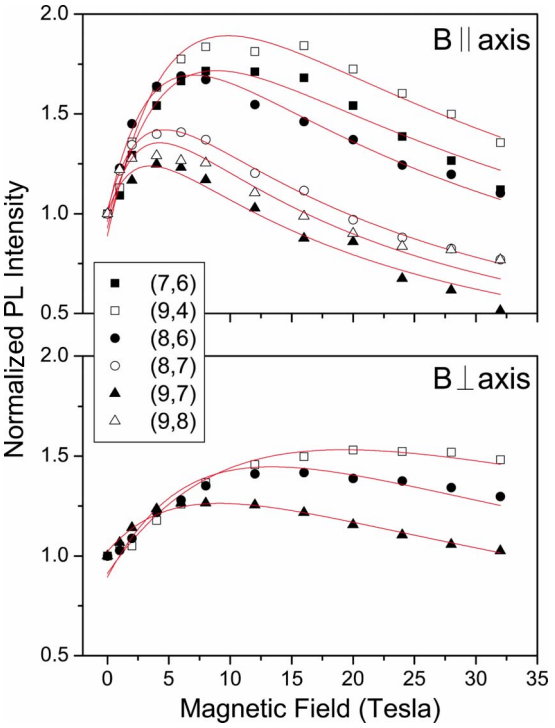

FIG. 3. (Color online) PL intensity for a range of nanotube species observed in the unstrained drop-cast MEHPPV film as a function of field. The use of polarized light allows the study of SWNTs oriented either parallel or perpendicular to the magnetic field.

finite intensity as $T \rightarrow 0$, which we model by assuming that there is a finite AB shift at $B=0$ of Δ_0. This has been treated in previous studies[14,16,21] where it has been attributed to disorder effects; however our analysis below suggests that there may be a more fundamental explanation for this term. The total AB shift is therefore given by

$$\Delta_{\mathrm{AB}} = \alpha B + \Delta_0. \tag{4}$$

Second there is clearly a systematic decrease in intensity with magnetic field. We model this by introducing an additional factor in the intensity $\sim 1/\Delta_{\mathrm{AB}}$ whose origin is yet to be explained. This gives a total intensity dependence on magnetic field of

$$I = \frac{\Delta_{\mathrm{AB}}^2}{\Delta_{\mathrm{AB}}^2 + \left[\frac{\Delta_x}{2} + \sqrt{\frac{\Delta_x^2}{4} + \Delta_{\mathrm{AB}}^2}\right]^2} \times \frac{A}{\Delta_{\mathrm{AB}}}, \tag{5}$$

where the amplitude A is a fitting constant. The emission energy dependence is given by

$$E = E_0 - \frac{\Delta_x \pm \sqrt{\Delta_x^2 + 4\Delta_{\mathrm{AB}}^2}}{2}, \tag{6}$$

where E_0 is the unperturbed transition energy. The measured magnetic-field-dependent intensities have been fitted to Eq. (5), which is found to give a good description of the observed data, and the energy dependence is fitted to Eq. (6). The values of α are mainly determined by the high-field dependence of E while the values for Δ_x come mainly from the intensity dependence. The values deduced for the dark–bright exciton splitting are shown in Fig. 4 and display two clear trends. First the values deduced for the drop-cast film, which has much less strain, are significantly lower (by a factor of ~ 0.7) than those deduced for the stretched polystyrene film. Second there is a clear diameter dependence in which the splitting increases rapidly as the diameter decreases. The values for the strained films are comparable to those reported recently by Shaver *et al.*[21] as deduced also from magnetic brightening for a few species in stretch aligned films. The values for the unstrained films are however much more similar to the values deduced from the temperature dependence of the emission from frozen solutions,[14] and to values deduced from measurements on individual nanotubes which have been recently reported.[33] The magnitude of all excitonic effects will be reduced somewhat due to our use of the polymer matrices to suspend the tubes as the larger local dielectric constant causes a significant[35] ($\sim 10\%$) reduction in the magnitude of Coulomb effects[9–12,35] relative to aqueous solutions. The larger effects produced by strain will influence the exciton binding energies through changes in the role of trigonal warping in the band structure which is known to influence the excitons.[4] The individual nanotube measurements show a very wide spread of values[33] even for the same species of tube but tend toward a large diameter tube result of ~ 2 meV as observed here. This suggests that, although environmental factors such as local dielectric constant or strain play a significant role in determining the exciton splitting as would be expected for Coulomb effects,[9–12,35] the large diameter limit may correspond to essentially degenerate bright and dark excitons.

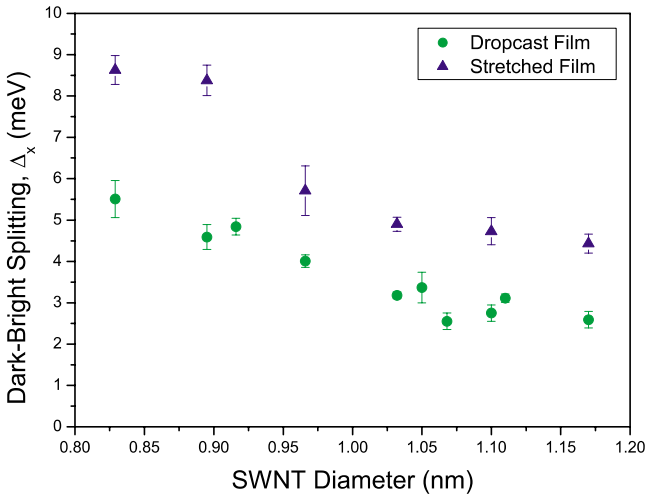

FIG. 4. (Color online) Dark–bright exciton splittings as deduced for light polarized parallel to the SWNT axis from fitting to Eq. (5).

The values for α are shown in Fig. 5 as a function of d, compared with the values expected theoretically using Eq. (1). The largest AB flux shift is measured when the tubes are aligned using the stretching and polarization parallel to the magnetic field ($\alpha_{\parallel}$), with values for $\alpha_{\perp}$ approximately half as large due to the partial alignment of the tubes. Significantly the intensity dependence on magnetic field (Fig. 3) is still accurately described by Eq. (5) with the same values of Δ_x

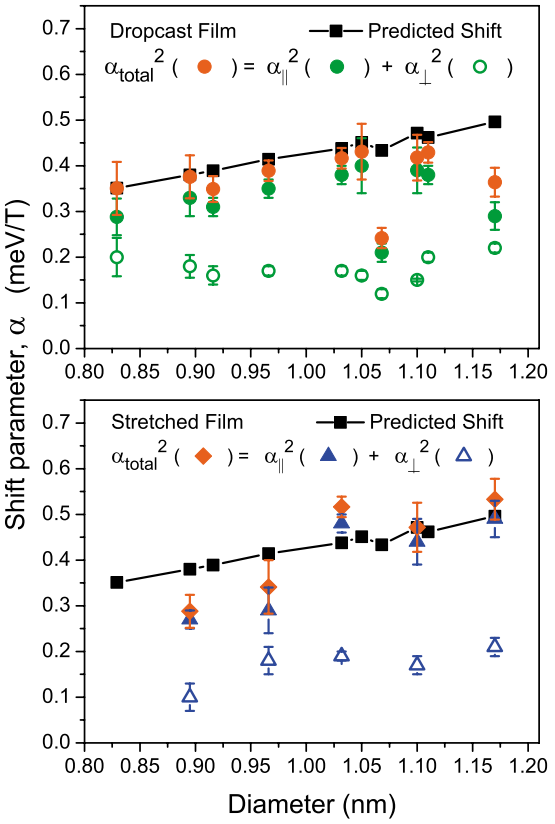

FIG. 5. (Color online) The values determined for the AB shift parameter, α, measured for different orientations for the different samples, compared with theoretically predicted values [Eq. (1)]. The geometrical sum of the parallel and perpendicular components, α_{total}, is found to be in good agreement with the theoretically predicted values.

for the perpendicular case provided that the equivalent value of $\alpha_\perp$ is used. This behavior allows us to estimate the total AB flux shift by geometrical summing of the shifts observed in the two polarizations, which are proportional to the two components of flux penetrating the tubes:

$$\alpha_{\text{total}} = \sqrt{\alpha_\parallel^2 + \alpha_\perp^2}, \tag{7}$$

as plotted in Fig. 5. This shows that the total AB shifts are in excellent agreement with the theoretically expected values[17] provided that the values used in Eq. (1) are the single-particle energy gaps[34,35] before Coulomb corrections are applied.

We now return to the high-field suppression of PL intensity. Previous reports have only seen a saturation of intensity[15,16,21] in the region of 20–60 T. The reason why the suppression of PL intensity is observable in the present work is because this behavior is only observed in the low-temperature, very high-field limit $\Delta_{\text{AB}} \gg \Delta_x$. This is accessed in the present study by the study of large diameter and unstrained samples which have smaller values of Δ_x and larger values of Δ_{AB}. In addition there is a reduction in Coulomb effects due to the higher dielectric constant in polymer matrix samples[35] which will also reduce Δ_x. The fact that the suppression scales with the component of flux threading the

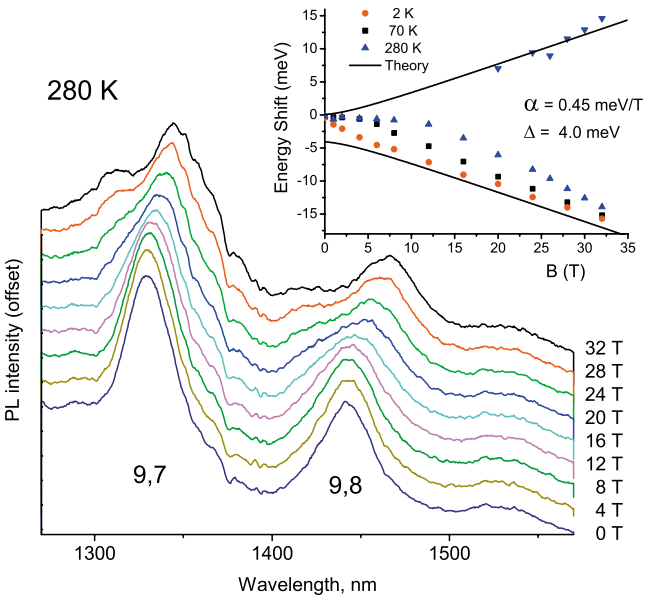

FIG. 6. (Color online) The PL spectra at 280 K from the stretched MEH-PPV films aligned parallel to the magnetic field studied from 0 to 32 T, excited at 820 nm. The inset shows the magnetic-field dependence of the peak shifts for the (9,8) peak, measured at 2, 70, and 280 K, compared with the predictions of Eq. (6) and the values of α and Δ_x deduced previously.

tubes, as shown by Fig. 3, suggests strongly that the suppression is related to the AB flux induced change in the exciton states[9] and not to any field dependent change in exciton transport processes which might influence the recombination time. Further evidence of the universality of this behavior is shown in Fig. 6 which shows a series of PL measurements at 280 K. The spectra show a clear AB splitting of the (9,7) and (9,8) peaks into two components at high field, and comparison of the field dependent shifts at 280 and 4 K (inset) shows that there is good agreement between the shifts deduced from the low-temperature behavior and the splitting observed at high temperature. Although the larger background present at 280 K makes a quantitative analysis of the intensity more uncertain, it is clear that the intensities of both components are significantly smaller at high field compared to $B=0$, again consistent with the idea that the field dependent suppression of intensity is related to the AB splitting and not to any population effects.

The origin of the magnetic-field-dependent suppression remains unclear; however, it can be noted that the high-field limit $\Delta_{\text{AB}} \gg \Delta_x$ corresponds to the formation of fully "valley polarized" exciton states which will be in reverse order for the E_1 and E_2 bands which might lead to inhibited interband relaxation to the lowest energy radiative states.

One further parameter which emerges from the analysis is the zero-field AB splitting Δ_0 which causes the zero-field intensity to be nonzero. Previous interpretations of this phenomenon as due to disorder do not give such a good description of the data as any disorder induced mixing of the bright and dark states only changes once the AB splitting is comparable to the disorder term, whereas all of the data observed here have a very strong, linear, field dependence at low field. This suggests that the AB splitting is added to an existing

zero-field splitting. A good candidate for this is the presence of a small spin-orbit splitting in the nanotubes, as suggested by Ando.[36] It was shown that the presence of a finite spin-orbit interaction in graphene, assumed to be of the same order as that found in diamond[37] (6 meV), would be equivalent to the addition of an Aharanov-Bohm phase of order $2\delta p\sigma$, where $\sigma = \pm 1$. The dimensionless parameters δ and p are directly related to the interband matrix elements and spin-orbit interaction, and have been estimated by Ando[36] to be of order of $10^{-2}-10^{-3}$ and 0.05. We find that all of the data fitted here can be well described using a value of $\Delta_0 = 1 \pm 0.3$ meV including both the strained and unstrained films. This value would correspond to a value of δ of order of 3×10^{-3}, consistent with the theoretical estimations.

IV. CONCLUSIONS

In summary therefore we have shown that the bright–dark exciton splittings in single-walled carbon nanotubes are strongly dependent on the strain state and local environment of the nanotubes. Large diameter, unstrained nanotubes have very small splittings, which are of the order of 2–3 meV, suggesting that the large diameter limit may tend toward degeneracy between the two states. The small splittings allow us to access a previously unknown high-field limit in which the PL intensity is found to be suppressed by high magnetic fields. This behavior had not been previously expected. Finally we observe evidence for a small zero-field AB splitting which we suggest may be related to spin-orbit splitting in graphene.

ACKNOWLEDGMENTS

Part of this work has been supported by EuroMagNET under the EU Contract No. RII3-CT-2004-506239 of the 6th Framework "Structuring the European Research Area, Research Infrastructures Action," and by the EPSRC-GB Basic Technology Grant scheme.

*r.nicholas1@physics.ox.ac.uk

[1] C. D. Spataru, S. Ismail-Beigi, L. X. Benedict, and S. G. Louie, Phys. Rev. Lett. **92**, 077402 (2004).
[2] C. D. Spataru, S. Ismail-Beigi, L. X. Benedict, and S. G. Louie, Appl. Phys. A: Mater. Sci. Process. **78**, 1129 (2004).
[3] V. Perebeinos, J. Tersoff, and P. Avouris, Phys. Rev. Lett. **92**, 257402 (2004).
[4] J. Jiang, R. Saito, Ge G. Samsonidze, A. Jorio, S. G. Chou, G. Dresselhaus, and M. S. Dresselhaus, Phys. Rev. B **75**, 035407 (2007).
[5] Y.-Z. Ma, L. Valkunas, S. M. Bachilo, and G. R. Fleming, J. Phys. Chem. B **109**, 15671 (2005).
[6] F. Wang, G. Dukovic, L. E. Brus, and T. F. Heinz, Science **308**, 838 (2005).
[7] J. Maultzsch, R. Pomraenke, S. Reich, E. Chang, D. Prezzi, A. Ruini, E. Molinari, M. S. Strano, C. Thomsen, and C. Lienau, Phys. Rev. B **72**, 241402(R) (2005).
[8] L.-J. Li, A. N. Khlobystov, J. G. Wiltshire, G. A. D. Briggs, and R. J. Nicholas, Nat. Mater. **4**, 481 (2005).
[9] T. Ando, J. Phys. Soc. Jpn. **75**, 024707 (2006).
[10] H. Zhao, S. Mazumdar, C.-X. Sheng, M. Tong, and Z. V. Vardeny, Phys. Rev. B **73**, 075403 (2006).
[11] C. D. Spataru, S. Ismail-Beigi, R. B. Capaz, and S. G. Louie, Phys. Rev. Lett. **95**, 247402 (2005).
[12] V. Perebeinos, J. Tersoff, and P. Avouris, Nano Lett. **5**, 2495 (2005).
[13] O. Kiowski, K. Arnold, S. Lebedkin, F. Hennrich, and M. M. Kappes, Phys. Rev. Lett. **99**, 237402 (2007).
[14] I. B. Mortimer and R. J. Nicholas, Phys. Rev. Lett. **98**, 027404 (2007).
[15] S. Zaric *et al.*, Phys. Rev. Lett. **96**, 016406 (2006).
[16] I. B. Mortimer, L.-J. Li, R. A. Taylor, G. L. J. A. Rikken, O. Portugall, and R. J. Nicholas, Phys. Rev. B **76**, 085404 (2007).
[17] H. Ajiki and T. Ando, J. Phys. Soc. Jpn. **62**, 1255 (1993).
[18] S. Roche, G. Dresselhaus, M. S. Dresselhaus, and R. Saito, Phys. Rev. B **62**, 16092 (2000).
[19] F. L. Shyu, C. P. Chang, R. B. Chen, C. W. Chiu, and M. F. Lin, Phys. Rev. B **67**, 045405 (2003).
[20] S. Zaric, G. N. Ostojic, J. Kono, J. Shaver, V. C. Moore, M. S. Strano, R. H. Hauge, R. E. Smalley, and X. Wei, Science **304**, 1129 (2004).
[21] J. Shaver, J. Kono, O. Portugall, V. Krstić, G. L. J. A. Rikken, Y. Miyauchi, S. Maruyama, and V. Perebeinos, Nano Lett. **7**, 1851 (2007).
[22] A. Nish, J. Y. Hwang, J. Doig, and R. J. Nicholas, Nat. Nanotechnol. **2**, 640 (2007).
[23] A. Nish, J. Y. Hwang, J. Doig, and R. J. Nicholas, Nanotechnology **19**, 095603 (2008).
[24] J. Y. Hwang, A. Nish, J. Doig, S. Douven, C. W. Chen, L. C. Chen, and R. J. Nicholas, J. Am. Chem. Soc. **130**, 3543 (2008).
[25] J. Shaver, S. A. Crooker, J. A. Fagan, E. K. Hobbie, N. Ubrig, O. Portugall, V. Perebeinos, P. Avouris, and J. Kono, Phys. Rev. B **78**, 081402(R) (2008).
[26] H. Ajiki, Phys. Rev. B **65**, 233409 (2002).
[27] J. Lefebvre, J. M. Fraser, P. Finnie, and Y. Homma, Phys. Rev. B **69**, 075403 (2004).
[28] R. S. Deacon, K. C. Chuang, J. Doig, I. B. Mortimer, and R. J. Nicholas, Phys. Rev. B **74**, 201402(R) (2006).
[29] L. Yang and J. Han, Phys. Rev. Lett. **85**, 154 (2000).
[30] L.-J. Li, R. J. Nicholas, R. S. Deacon, and P. A. Shields, Phys. Rev. Lett. **93**, 156104 (2004).
[31] T. K. Leeuw, D. A. Tsyboulski, P. N. Nikolaev, S. M. Bachilo, S. Arepalli and R. B. Weisman, Nano Lett. **8**, 826 (2008).
[32] K. Arnold, S. Lebedkin, O. Kiowski, F. Hennrich, and M. M. Kappes, Nano Lett. **4**, 2349 (2004).
[33] A. Srivastava, H. Htoon, V. Klimov, and J. Kono, Phys. Rev. Lett. **101**, 087402 (2008).
[34] V. N. Popov New, J. Phys. **6**, 17 (2004).
[35] K.-C. Chuang, A. Nish, J. Y. Hwang, G. W. Evans, and R. J. Nicholas, Phys. Rev. B **78**, 085411 (2008).
[36] T. Ando, J. Phys. Soc. Jpn. **69**, 1757 (2000).
[37] C. Rauch, *Proceedings International Conference on Physics of Semiconductors* (Institute of Physics, London, 1962).